ELSEVIER

Effect of magnesium on preferential oxidation of carbon monoxide on platinum catalyst in hydrogen-rich stream

Sung-Ho Cho [a,*], Jong-Soo Park [b], Seung-Hoon Choi [c], Sung-Hyun Kim [a,**]

[a] Department of Chemical and Biological Engineering, Korea University, 1 Anam-Dong, Sungbuk-Ku, Seoul 136-701, Republic of Korea
[b] Conversion Process Research Center, Korea Institute of Energy Research, P.O. Box 103, Yusong-Ku, Taejon 305-600, Republic of Korea
[c] Department of Environmental and Chemical Engineering, Seonam University, Gwangchi-Dong, Namwon-city, Jeonbuk 590-711, Republic of Korea

Abstract

The effects of magnesium on platinum catalyst used for the preferential oxidation of carbon monoxide for polymer electrolyte membrane fuel cell applications are investigated. The CO conversion and selectivity on Pt–Mg/Al$_2$O$_3$ for a H$_2$-rich stream are 93.1 and 62.0%, respectively, but only 70.2 and 46.89% on Pt/Al$_2$O$_3$. The superior activity of Pt–Mg/Al$_2$O$_3$ for the preferential oxidation of CO is due to an increase in the hydroxyl groups that results from an increase in basicity with the addition of Mg, as well as to an increase in the electron density on the surface of the Pt catalyst. Moreover, the content of hydroxyl groups on the Pt catalysts is promoted by water vapour.

1. Introduction

The fuel cell is a prospective replacement for the conventional internal-combustion engine, because it offers greater efficiency and does not discharge pollutants into the atmosphere [1]. With respect to stationary applications, polymer electrolyte membrane fuel cells (PEMFCs) fuelled by hydrogen appear to be the most promising option for residential power generation (RPG) facilities due to their compactness, modularity, high power density, energy efficiency, and fast response [2]. Because of challenges, such as storage and delivery when hydrogen is used directly as a primary fuel, extensive research has been directed towards the development of systems for hydrocarbon reforming to generate hydrogen.

Reformate gases produced by reforming include significant amounts of CO. Migration of CO to the fuel cell stack reduces the efficiency of electricity production. In practice,

the CO content in fuel gas mixture must be kept below 100 ppm [3]. Preferential oxidation (PrOx) is one method for removing CO. Many efforts have been made to improve the activity of the Pt catalyst used in the PrOx process [4]. It is generally known that the selectivity of Pt/Al$_2$O$_3$ is low. For example, more than twice the amount of oxygen has to be added to remove 1.0% CO completely [5].

The activity of the Pt catalyst for the PrOx reaction can be improved by the addition of a transition metal (Fe, Sn, Co, and Ce) [6–9]. Unfortunately, CO conversion over these catalysts is dramatically decreased at high temperature (<150 °C), and maximum CO conversion occurs at a relatively low temperature (≥100 °C). Moreover, these promoters do not improve the selectivity.

In a fuel processor, the PrOx reactor is linked with a reforming reactor and a water–gas shift reactor. Therefore, PrOx must be operated with consideration to energy balance of the whole fuel processor. Although, there will be differences according to the type of system, a PrOx reactor might be operated at 130–200 °C in a conventional reformer [10].

It is known that the activity and the selectivity of precious metal catalyst increase in the presence of alkali metal.

* Corresponding author. Tel.: +82 42 860 3667; fax: +82 42 860 3134.
** Co-corresponding author. Tel.: +82 2 3290 3297.
E-mail addresses: cho0903@korea.ac.kr (S.-H. Cho), kimsh@korea.ac.kr (S.-H. Kim).

For example, Tanaka et al. [11,12] reported that CO conversion and selectivity over K-Rh/USY was higher than that over Rh/USY for the PrOx reaction. The cause of such improvement in activity and selectivity by alkali metals can be explained by interaction between CO and precious metal. Alkali metals increase this interaction so that the CO content on the catalyst becomes high. Also, the electron density of the precious metal is increased by electron transfer form the alkali metal to the precious metal.

The oxidation of CO over a Pt catalyst proceeds in hydrogen-rich stream by a low-rate branched mechanism. Because adsorbed CO blocks oxygen adsorption (oxygen adsorption is the rate-determining step), the rate of CO oxidation can decrease with increasing strength of this interaction. Nevertheless, the activity for CO oxidation of a catalyst containing an alkali metal is excellent at low temperature.

The effect of alkali metal on CO oxidation in a hydrogen-rich gas, such as that used in PrOx, has still to be fully elucidated. We have tried to understand how alkali metal affects the activity of precious metal catalysts in the PrOx reaction. In this research, we conducted experiments with Pt/Al_2O_3.

2. Experimental

2.1. Preparation and characterization of catalyst

Al_2O_3 power (5 g) was contacted with an aqueous solution of H_2PtCl_6 (Aldrich Co.), followed by drying at $100\,^\circ C$ for 24 h. The dried catalyst powder was calcined at $400\,^\circ C$ for 4 h. The promoted $Pt–Mg/Al_2O_3$ catalysts were prepared by incipient wetness impregnation with an aqueous solution of H_2PtCl_6 and $Mg(NO_3)_3·6H_2O$ (Aldrich Co.). The $Pt–Mg/Al_2O_3$ catalysts were dried and calcined by the same method. The metal contents and physical properties of the catalysts are shown in Table 1.

H_2-TPR and CO_2-TPD tests were carried out using an Autochem 2910 instrument (Micromeritics Co.) equipped with a thermal conductivity detector. Before the TPR test, the catalyst was reduced at $300\,^\circ C$ for 2 h and oxidized in the atmosphere at $400\,^\circ C$ for 0.5 h. The change in hydrogen concentration in the reactants was measured for an increase in temperature from -50 to $400\,^\circ C$ at a rate of $2\,^\circ C\,min^{-1}$ in a hydrogen flow atmosphere of 5.0 vol.% H_2/Ar.

X-ray photoelectron spectroscopy (XPS) analyses were performed with a ESCALAB MK-2 (VG Scientific Ltd.) spectrometer with a Mg Kα anode (1253.6 eV) at an accelera-

tion voltage of 13 kV and current of 20 mA. Charging effects were corrected by adjusting the C1s peak to a position of 285.0 eV. Freshly-prepared catalysts were analyzed first by a wide-scan of 0–1100 eV binding energy and then by single-scan analysis of the Pt $4d_{5/2}$ regions.

In order to analyze the type of adsorbed CO on the Pt catalysts, an experiment was carried out using an FT/IR-660 (JASCO Inc.) instrument equipped with a MCT narrow band detector. After the reduced powder catalyst (0.1 g) was put in the reaction cell, it was pretreated with He at $300\,^\circ C$ for 2 h. The He was passed into the reaction cell at a rate of $30\,ml\,min^{-1}$. Through this experiment, the effects of oxygen and moisture on CO adsorption were examined using the following different compositions of reactants: (i) 0.4 vol.% CO/He, (ii) 0.4 vol.% CO/He + 0.8 vol.% H_2O/He.

2.2. Experimental procedure

The catalytic activity was measured in a micro-fixed bed reactor. The micro-reactor was a quartz tube of 6 mm in internal diameter and 50 mm in length. Air, H_2, CO_2, 20% CO (N_2 balance) were used as-received without further purification. Water was introduced from the vaporization chamber. The catalyst loading was 0.1 g and the flow rate was set at 100 ml (STP) min^{-1}. The activity of the catalysts was examined at $130–230\,^\circ C$.

3. Results

3.1. Characterization of Pt catalysts

3.1.1. Basicity

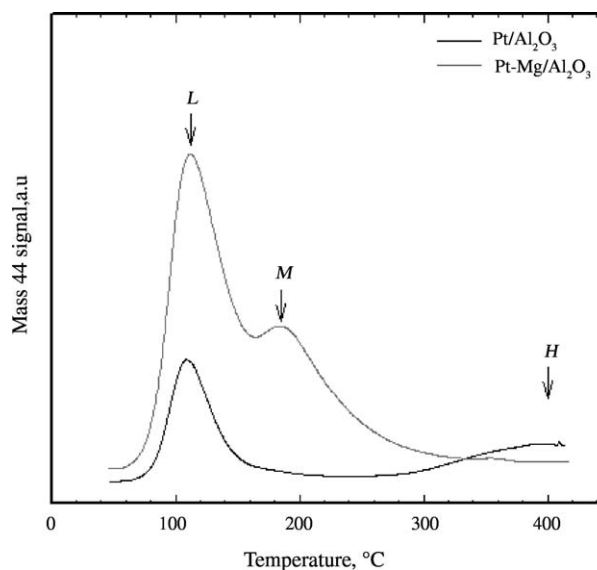The basicity of Pt/Al_2O_3 and $Pt–Mg/Al_2O_3$ was measured by means of CO_2-TPD and the results are shown the Fig. 1.

Table 1
Metal content and physical properties of Pt/Al_2O_3 and $Pt–Mg/Al_2O_3$

Catalyst	Pt (wt.%)	Mg (wt.%)	BET ($m^2\,g^{-1}$)	Pt dispersion (%)[a]
Pt/Al_2O_3	2.0	0.0	155.8	31
$Pt–Mg/Al_2O_3$	2.0	3.0	141.6	28

[a] Calculated by H_2 chemisorption.

Fig. 1. CO_2-TPR pattern for Pt/Al_2O_3 and $Pt-Mg/Al_2O_3$.

The temperature range of CO_2 desorption is divided into three regions as follows: low basicity sites (L) where CO_2 is desorbed within the range of 80–140 °C; medium basicity sites (M) where CO_2 is desorbed within the range of 160–240 °C; high basicity sites (H) where CO_2 is desorbed at over 300 °C.

It was generally recognized that this difference in desorption temperature is due to the basic strength of the catalyst surface [13–15]. For example, CO_2 adsorbed on low basicity sites, which are related to OH^- groups on the catalyst, is desorbed at around 100 °C, while CO_2 on absorbed the medium strength and strong basicty sites desorbs at 180–250 and 275–500 °C, respectively. Here, the medium strength of basicity is related to the oxygenated ion of Mg^{2+}–O^{2-} and $2Al^{3+}$–$3O^{2-}$, and the strong basicity is associated with the isolated O_2^- in the lattice of MgO [15].

In our experiments, the profile for CO_2-TPD on each Pt catalyst was different although these catalysts had been pre-treated with the same method. Thus, low basicity (L) and high basicity (H) were observed with Pt/Al_2O_3 catalysts, but the concentration of low basicity sites (L) for $Pt–Mg/Al_2O_3$ catalysts containing Mg was higher than that for Pt/Al_2O_3 and medium basicity sites (M) were detected.

3.1.2. Oxidized state of Pt catalysts

The oxidized state of Pt in Pt/Al_2O_3 and $Pt–Mg/Al_2O_3$ was measured by XPS. The catalysts were reduced with H_2 at 300 °C for 2 h before XPS analysis and the results are shown in Fig. 2. The spectrum of Pt $4d_{5/2}$ was separated by means of the Gaussian–Lorentzian curve fitting method.

The Pt on the reduced Pt/Al_2O_3 and $Pt–Mg/Al_2O_3$ was mainly in the metallic state (Pt^0) and mono-oxidized state (PtO), but PtO_2 was not detected. The oxidized state of Pt for each catalyst was compared in terms of the ratio of the graphic area for PtO to that for Pt^0 (PtO/Pt^0). As shown in Fig. 2, the ratio of PtO/Pt^0 for Pt/Al_2O_3 and $Pt–Mg/Al_2O_3$ was 0.82 and 0.56, respectively. Thus, Pt on $Pt–Mg/Al_2O_3$ is more reduced than that on Pt/Al_2O_3. Incidentally, the electron density of Pt on $Pt–Mg/Al_2O_3$ is higher than that on Pt/Al_2O_3. With addition the Mg to the Pt catalyst, the electron density of Pt increases and it has been reported that the electron density of the catalyst is affected equally by various alkali metals [16].

The stability of Pt^0 on Pt/Al_2O_3 and $Pt–Mg/Al_2O_3$ was evaluated by the H_2-TPR method which measures the H_2 consumption with increasing temperature after the catalyst are oxidized at 400 °C for 2 h in air; the results are presented in Fig. 3. The H_2-TPR of Pt/Al_2O_3 has a H_2 consumption peak at around $T = 75$ °C. For the $Pt–Mg/Al_2O_3$ catalyst, two low and broad peaks at $T = -5$ and 80 °C are detected.

Hwang et al. [17] studied the variation of H_2 consumption temperature with the oxidized state of Pt on Pt/Al_2O_3 by the H_2-TPR method. It was reported that the H_2 consumption peak of physically adsorbed O_2 on Pt^0 was detected below 0 °C and that of oxygen on PtO and PtO_2 appeared at 50 and 100 °C, respectively.

Using the same procedure, the Pt^0 of $Pt–Mg/Al_2O_3$ was found to very stable, although it was contacted with oxygen at
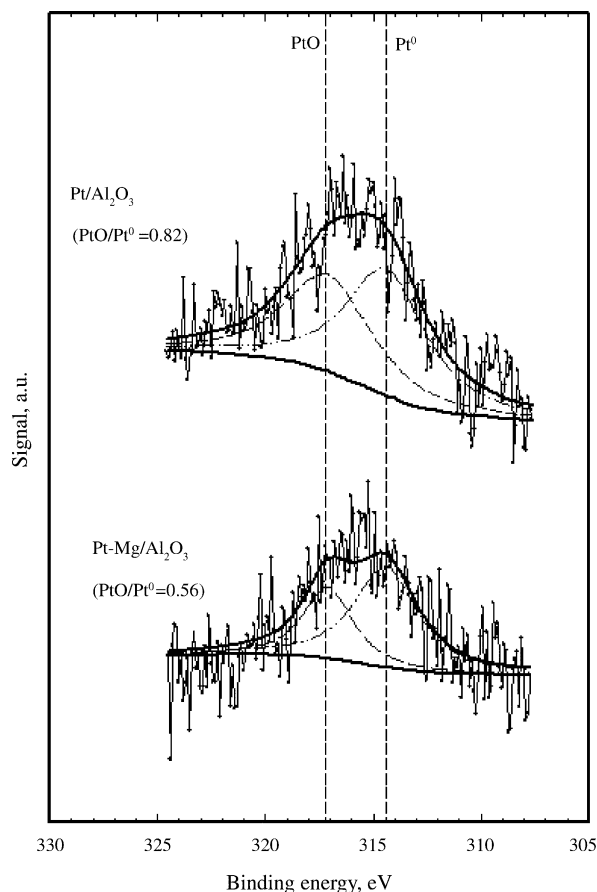

Fig. 2. Curve fitting of Pd $4d_{5/2}$ core level spectra for Pt/Al_2O_3 and $Pt–Mg/Al_2O_3$ catalysts reduced by H_2.

high temperature (400 °C). Since the ionization potential of metal oxide is reduced with increasing basicity of the catalyst [18], the stability of Pt^0 on $Pt–Mg/Al_2O_3$ originated form the increased basicity of the catalyst surface with Mg.
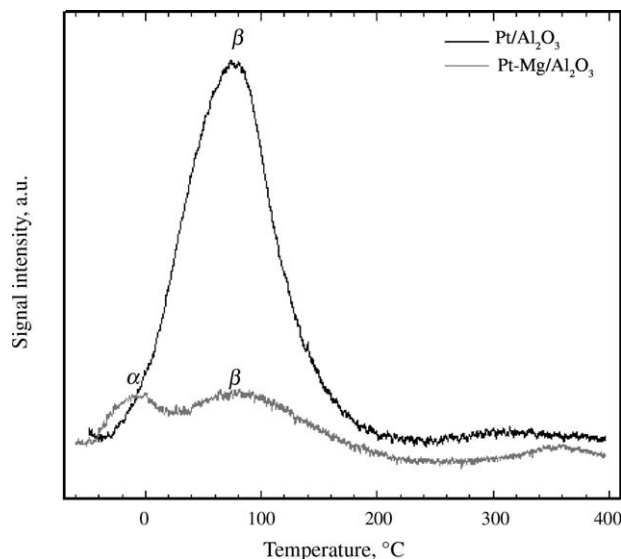

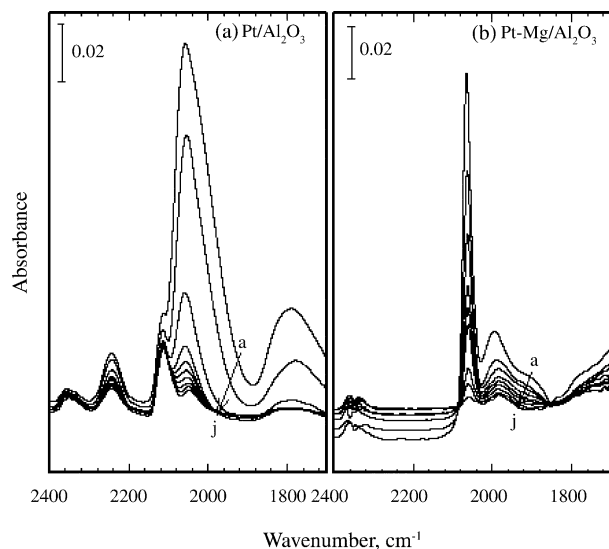Fig. 3. TPR patterns for Pt/Al_2O_3 and $Pt–Mg/Al_2O_3$.

Fig. 4. Variation of DRIFTS spectra of CO on Pt/Al$_2$O$_3$ and Pt–Mg/Al$_2$O$_3$ with desorption time at 250 °C. Desorption time: (a) 1 min, (b) 2 min, (c) 3 min, (d) 4 min, (e) 5 min, (f) 6 min, (g) 8 min, (h) 9 min, (i) 10 min, and (j) 11 min.

3.1.3. DRIFTS

DRIFTS was used to measure the effect of Mg on the type of adsorbed CO on the reduced Pt catalyst and the thermal stability. The experiment was conducted at 250 °C and atmospheric pressure. First, CO was adsorbed on the Pt catalyst at 250 °C for 30 min, subsequently a type of residual adsorbed CO was measured every 2 min with purging by He. The results are shown in Fig. 4.

In the IR spectra of Pt/Al$_2$O$_3$, two bands at 2124 and 2063 cm^{-1} are detected after 2 min. For the Pt–Mg/Al$_2$O$_3$ catalyst, two broad peaks at 2057 and 1996 cm^{-1} are detected. Most studies of CO/Pt systems show a band in the range of 2100–2200 cm^{-1}; that has been attributed to linearly-adsorbed CO on Pt atoms. Linearly-adsorbed CO on Pt/Al$_2$O$_3$ and Pt–Mg/Al$_2$O$_3$ displays a band at 2124 and 2057 cm^{-1}, respectively. These bands shift to lower frequency on increasing the desorption time. The band of linearly-adsorbed CO depends on the dipole–dipole interaction increasing with surface coverage [19] or on the degree of reduction of Pt [20]. In the IR experiments reported here for Pt/Al$_2$O$_3$ and Pt–Mg/Al$_2$O$_3$, the wavenumber of linearly-adsorbed CO on Pt–Mg/Al$_2$O$_3$ is higher than that on Pt/Al$_2$O$_3$. This is due to the degree of reduction of Pt, i.e. the amount of the metallic state in Pt–Mg/Al$_2$O$_3$ is higher than that in Pt/Al$_2$O$_3$, as shown by the XPS results.

On evaluating the thermal stability of adsorbed CO on Pt/Al$_2$O$_3$, the band detected at 2124 cm^{-1} is found to be stable at high temperature. This is attributed to the symmetric stretching of Pt$^{\delta+}$–(CO)$_2$ species [21]. For Pt–Mg/Al$_2$O$_3$, the band that appears at 1996 cm^{-1} is shifted to 1985 cm^{-1} with increasing desorption time. It has been reported that three different bands for CO adsorption on Pt supported
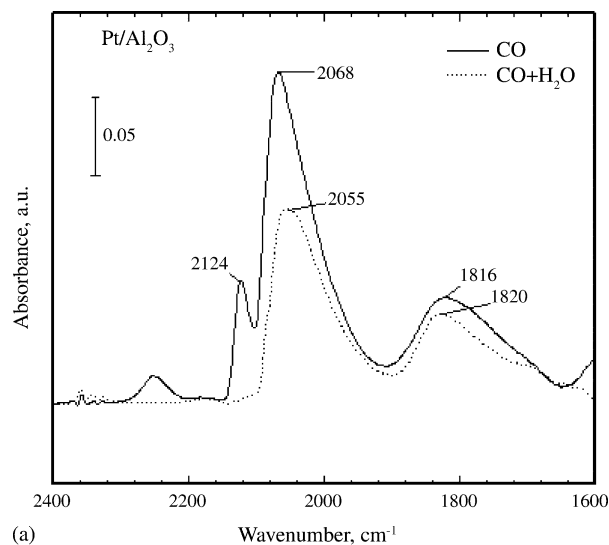
(a)
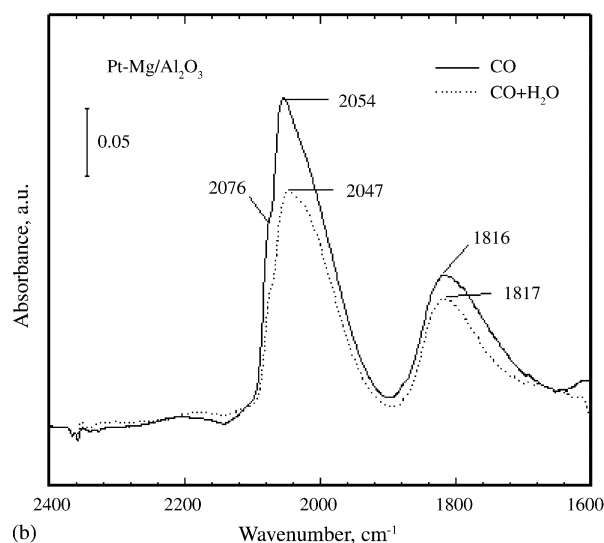
(b)

Fig. 5. Variation of infrared spectra of CO on Pt/Al$_2$O$_3$ and Pt–Mg/Al$_2$O$_3$ with water vapour at 100 °C.

over Mg–Al(O) occur in the range of 2020–1930 cm^{-1} [22,23]. It was concluded that the band at around 2000 cm^{-1} might be due to linearly-adsorbed CO on Pt sites of extremely low co-ordination. The band at 1930 cm^{-1} associated with bridge-bonded CO between Pt sites and Mg^{2+} or partially reduced Mg cations was not present on Pt–Mg/Al$_2$O$_3$.

Water vapour, which can be generated by hydrogen oxidation and included in feed stream, will participate in the PROX reaction. The effect of water vapour for CO adsorption on Pt catalysts was studied and the findings are presented in Fig. 5. For all catalysts, the bands of adsorbed CO are shifted to lower wavenumbers by water vapour. In particular, the thermally-stable band at around 2124 cm^{-1} for Pt/Al$_2$O$_3$ disappears when water vapour is in the feed stream.
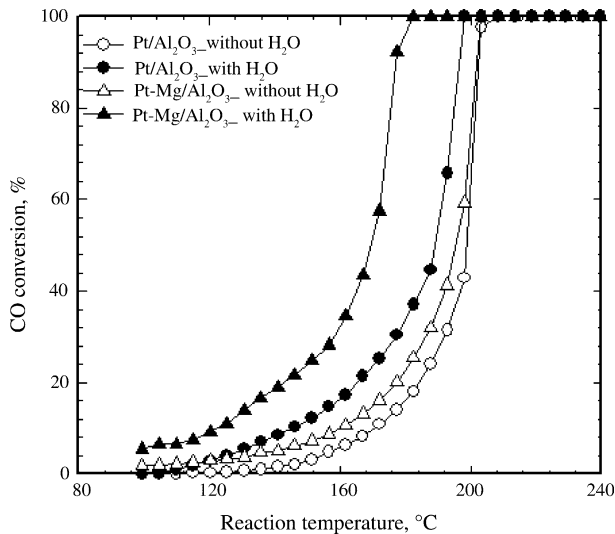
Fig. 6. Effect of water vapour on CO oxidation on Pt/Al_2O_3 and $Pt–Mg/Al_2O_3$. Reaction conditions: 1.0% CO, 0.75% O_2, 2.0% H_2O, rest N_2, GHSV = 60 000 h^{-1}.

3.2. Catalytic activity

3.2.1. CO oxidation

A comparison of the activities of Pt/Al_2O_3 and $Pt–Mg/Al_2O_3$ for CO oxidation was performed under both dry and wet conditions. In the feed stream, the O/CO ratio and the gas hourly specific velocity (GHSV) were fixed by 1.5 and 60 000 h^{-1}. The effects of magnesium and moisture on the catalytic activity for the CO oxidation reaction over Pt/Al_2O_3 and $Pt–Mg/Al_2O_3$ catalysts are shown in Fig. 6. Temperatures for CO conversion of 30% (T_{30}) and 50% (T_{50}) under dry conditions are 192 and 199 °C, respectively, for Pt/Al_2O_3 catalysts and 186 and 191 °C for $Pt–Mg/Al_2O_3$ catalysts. The activity of Pt/Al_2O_3 and $Pt–Mg/Al_2O_3$ catalysts is improved with reactants containing moisture. The T_{30} of 177 °C and T_{50} of 189 °C for the Pt/Al_2O_3 catalyst for moisture conditions are 2–9 °C lower than those for dry conditions. The CO oxidation activity of the $Pt–Mg/Al_2O_3$ catalysts for moist conditions is higher than that of Pt/Al_2O_3 catalysts, i.e. the T_{30} of 158 °C and T_{50} of 169 °C are about 20 °C lower than the valuses for dry conditions.

3.2.2. Preferential oxidation of CO in a H_2-rich stream

The activity of $Pt–Mg/Al_2O_3$ for the PrOx reaction has been compared with that of Pt/Al_2O_3 at O/CO = 1.5 and GHSV = 60 000 h^{-1}, see Fig. 7. The CO conversion and selectivity on Pt/Al_2O_3 have a maximum value at 200 °C, whereas those on $Pt–Mg/Al_2O_3$ reach a maximum at 170 °C. Moreover, the activity of $Pt–Mg/Al_2O_3$ is superior to that of Pt/Al_2O_3 in the range of 150–230 °C. The maximum values of CO conversion and selectivity for Pt/Al_2O_3 are 70.2 and 46.8%, respectively, at 200 °C, but those for $Pt–Mg/Al_2O_3$ are 93.1 and 62.0% at 170 °C. Hydrogen oxidation is a competitive reaction and thus the extent of CO conversion on all catalysts decreases above T_{max}.
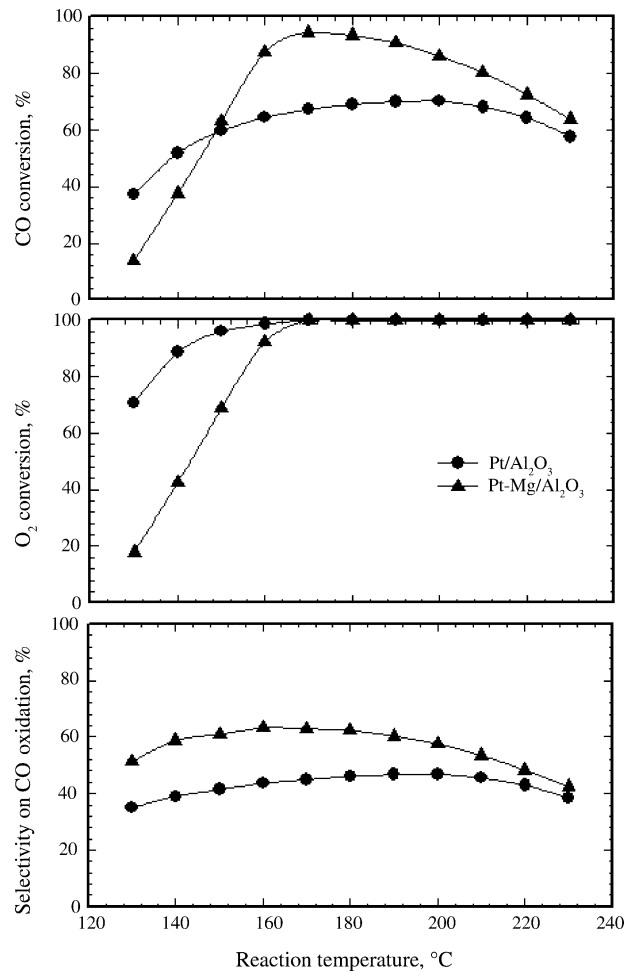

Fig. 7. Activity of Pt/Al_2O_3 and $Pt–Mg/Al_2O_3$ for preferential oxidation of CO in H_2-rich stream. Reaction conditions: 1.0% CO, 0.75% O_2, 20.0% CO_2, 65.0% H_2, 2.0% H_2O, rest N_2, GHSV = 60 000 h^{-1}.

3.2.3. Effects of water vapour and CO_2 content on PrOx over $Pt–Mg/Al_2O_3$

The H_2-rich stream generated through hydrocarbon or alcohol reforming includes about 10–20 vol.% water vapour and about 20 vol.% CO_2 and these compositions except an influence on the activity of the catalyst for the PrOx [24]. The effect of water vapour and CO_2 on PrOx over $Pt–Mg/Al_2O_3$ is presented in Fig. 8. At 100 °C, CO conversion and selectivity are 30.2 and 74.3% for conditions without CO_2 and water vapour, but these fall to, respectively, 7.5 and 51.4% in the presence of 20.0 vol.% CO_2. By contrast, O_2 conversion is improved with increasing water vapour content in the feed stream. The selectivity is highest at 66.6% with 2.0 vol.% water vapour injection. The maximum CO conversion and selectivity are shown at 170 °C under all conditions. CO conversion and selectivity fall from 99.5 and 66.3 to 94.6 and 63.0% with 20.0 vol.% CO_2 under dry conditions. On injecting 2.0 vol.% water vapour, CO conversion and selectivity are increased to 98.0 and 67.3% at 170 °C, but decreases to 87.9 and 58.6% with 10.0 vol.% water vapour.
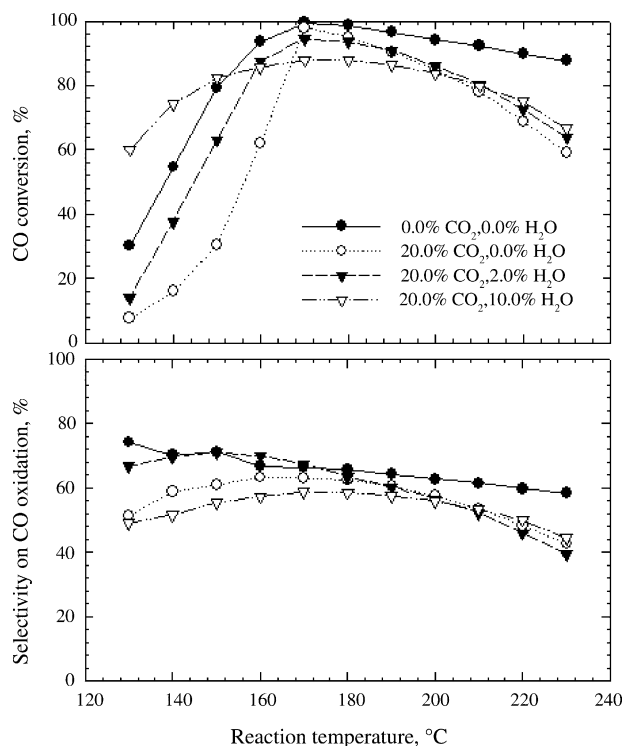
Fig. 8. Effect of CO_2 and H_2O on preferential oxidation of CO over Pt–Mg/Al_2O_3 in H_2-rich stream. Reaction conditions: 1.0% CO, 0.75% O_2, 20.0% CO_2, 65.0% H_2, rest N_2, GHSV = 60 000 h^{-1}.

4. Discussion

As shown from the results for CO oxidation (Fig. 6) and PrOx (Fig. 7), the activity of Pt–Mg/Al_2O_3 is higher than that of Pt/Al_2O_3 (note, for CO oxidation under dry conditions, the activity of Pt/Al_2O_3 is little improved with Mg). This improvement results from the difference in the oxidative state of Pt on each catalyst. According to previous research [16], the interaction strength between Pt and CO decreases with decrease in the oxidation state of Pt. If compared, however, with the results for humid conditions, water vapour improves the oxidation rate over the Pt catalyst than does the oxidative state of Pt itself. It has already been reported [1,25] that the oxidation rate is increased by the hydroxyl groups which originate from water vapour that is adsorbed.

According to the mechanism proposed by Costello et al. [26], hydroxyl groups (OH^-) are produced on noble metals with low electron density. These hydroxyl groups react with CO to form hydroxycarbonyl. In this reaction, oxygen is easily dissociated and adsorbed on noble metals with high electron density. In this study, oxidation occurrs through a mechanism in which dissociation-adsorbed oxygen atoms react with hydroxycarbonyl and produce CO_2. CO oxidation over Pt/Al_2O_3 progresses though the same route, as shown in Fig. 5.

The electron density of Pt in Pt–Mg/Al_2O_3 is higher than that in Pt/Al_2O_3, and $Pt^{\delta+}$–$(CO)_2$ is not generated under all conditions, as shown in Fig. 5. The superior activity

of Pt–Mg/Al_2O_3 under humid conditions results from the promoted basicity with Mg. The concentration of hydroxyl groups is increased with increasing basicity on the catalyst surface under humid conditions. Considering the above results, the oxidation rate on Pt is influenced more by the concentration of hydroxyl group.

Nevertheless, CO conversion and selectivity on Pt–Mg/Al_2O_3 for the PrOx reaction are superior to those on Pt/Al_2O_3. The data from XPS analyses show that the Pt^0 concentration on Pt–Mg/Al_2O_3 is higher than that on Pt/Al_2O_3. The electron density on the surface of Pt–Mg/Al_2O_3 is also higher than that of Pt/Al_2O_3, as indicated in Fig. 4 and is influenced by water vapour. The electron is supplied from the magnesium to the active metal in the catalyst and the strengthens CO adsorption [27,28].

5. Conclusions

The present study has examined the effects of Mg on the activity of Pt catalysts for the preferential oxidation of CO. Pt–Mg/Al_2O_3 catalysts are superior to Pt/Al_2O_3 catalysts in a H_2-rich stream due to two reasons first, basicity improved by the addition of Mg enhances the concentration of hydroxyl groups on the surface of Pt catalysts, and increases reaction activity. Nevertheless, the selectivity of Pt–Mg/Al_2O_3 for preferential oxidation of CO is decreased on increasing the content of water vapour in feed stream, which prevents CO from being adsorbed into the surface of Pt metal. Second, the CO concentration on Pt–Mg/Al_2O_3 is higher than that on Pt in Pt/Al_2O_3, because the electron density on the surface of Pt–Mg/Al_2O_3 is increased by the addition of Mg.

Acknowledgments

References

[1] M.J. Kahlich, H.A. Gasteiger, R.J. Behm, J. Catal. 171 (1997) 93.
[2] T.R. Ralph, Platinum Met. Rev. 43 (1999) 14.
[3] H.-F. Oetjen, V.M. Schmidt, U. Stimming, F. Trila, J. Electrochem. Soc. 143 (1996) 3838.
[4] J.G.E. Cohn, US Patent 3,216,782, November 9 (1965).
[5] A. Manasilp, E. Gulari, Appl. Catal. B 37 (2002) 17.
[6] O. Korotkikh, R. Farrauto, Catal. Today 62 (2000) 249.
[7] A. Wootsch, C. Bescorme, D. Duprez, J. Catal. 225 (2004) 259.
[8] C. Özdemir, A.N. Akm, R. Yildirim, Appl. Catal. A 258 (2004) 145.
[9] W.S. Epling, P.K. Cheekatamarla, A.M. Lane, Chem. Eng. J. 93 (2003) 61.
[10] C.D. Dudfield, R. Chen, P.L. Adcock, Int. J. Hydrogen Energ. 26 (2001) 763.

[11] H. Tanaka, S.-I. Ito, S. Kameoka, K. Tomishige, K. Kunimori, Catal. Commun. 4 (2003) 1–4.

[12] H. Tanaka, S.-I. Ito, S. Kameoka, K. Tomishige, K. Kunimori, Appl. Catal. A 250 (2003) 255.

[13] F. Cavani, F. Trifirò, A. Vaccari, Catal. Today 11 (1991) 173.

[14] D. Tichit, M.H. Llhouty, A. Guida, B.H. Chiche, F. Figueras, A. Auroux, D. Bartalini, E. Garrone, J. Catal. 151 (1995) 50.

[15] M. Bolognini, F. Cavani, D. Scagliarini, C. Flego, C. Perego, M. Saba, Catal. Today 75 (2002) 103.

[16] H.J. Kreuzer, R.L.C. Wang, Z. Phys. Chem. 202 (1997) 127.

[17] C.P. Hwang, C.T. Yeh, J. Mol. Catal. A: Chem. 112 (1996) 295.

[18] B.L. Mojet, J.T. Miller, D.E. Ramaker, D.C. Koningsberger, J. Catal. 186 (1999) 373.

[19] F. Stoop, F.J.C. Toolenaar, V. Ponec, J. Catal. 73 (1982) 50.

[20] C. Hippe, R. Lamber, G. Schultz-Ekloff, U. Schubert, Catal. Lett. 43 (1997) 195.

[21] A.Yu. Stakheev, E.S. Shpiro, O.P. Tkachenko, N.I. Jaeger, G. Schulz-Ekloff, J. Catal. 169 (1997) 382.

[22] G.S. Lane, J.T. Miller, F.S. Modica, M.K. Barr, J. Catal. 141 (1993) 465.

[23] Z. Gandao, B. Coq, L.C. de Ménorval, D. Tichit, Appl. Catal. A 147 (1996) 395.

[24] M.M. Schubert, A. Venugopal, M.J. Kahlich, V. Plzak, R.J. Behm, J. Catal. 222 (2004) 32.

[25] H. Muraki, S.I. Matunaga, H. Shinjoh, M.S. Wainwright, D.L. Trimm, J. Chem. Tech. Biotechnol. 52 (1991) 415.

[26] C.K. Costello, M.C. Kung, H.S. Oh, Y. Wang, H.H. Kung, Appl. Catal. A 232 (2002) 159.

[27] N. Pavlenko, P.P. Kostrobij, Y. Suchorski, R. Imbihl, Surf. Sci. 489 (2001) 29.

[28] L.F. Liotta, G.A. Martin, G. Deganello, J. Catal. 164 (1996) 322.